J Infrared Milli Terahz Waves (2018) 39:840–853
https://doi.org/10.1007/s10762-018-0513-3

A Comprehensive Study of Albumin Solutions in the Extended Terahertz Frequency Range

M. M. Nazarov[1] · **O. P. Cherkasova**[2,3] · **A. P. Shkurinov**[4,5]

Received: 27 February 2018 / Accepted: 20 June 2018 / Published online: 30 June 2018

Abstract Sensitivity of the THz frequency range to the solutions of biomolecules originates from the decrease of absorption and dispersion of water in its bound state. Correct measurement and interpretation of the THz spectra of water-containing samples is still a challenging task because the reliable relaxation model for such spectra is not well established. The transmission and the attenuated total internal reflection geometries data were combined for precise analysis of the spectra of the aqueous solutions of bovine serum albumin within the range 0.05–3.2 THz. We compare the concentration dependencies of the dielectric function at "low," "middle," and "high" frequency and do not confirm an anomalous increase in absorption for concentrations below 17 mg/mL published by other teams.

Keywords Terahertz time-domain spectroscopy · Transmission · Attenuated total internal reflection · Protein solution · Water · BSA · Relaxation model

1 Introduction

The terahertz sensing of protein solutions has a fundamental scientific (a) and applied (b) significance: (a) the studies of the collective motion of water molecules around protein ones and determination of the size of the protein hydration shell; (b) analysis of protein

✉ M. M. Nazarov
o.p.cherkasova@gmail.com

[1] National Research Center, Kurchatov Institute, Moscow 123182, Russia

[2] Institute of Laser Physics of SB RAS, Novosibirsk 630090, Russia

[3] Tomsk State University, Tomsk 634050, Russia

[4] Crystallography and Photonics Federal Research Center, Russian Academy of Sciences, Moskva, Russia

[5] Lomonosov Moscow State University, Moscow 119991, Russia

concentration in solution in pharmacological and medical studies. In aqueous environment, proteins demonstrate their most important biological functions. Up to now, a large amount of data relating to the nature of protein dissolution in aqueous solutions has been collected. Fundamental results are obtained on the interaction of water molecules with dissolved proteins, and it is established that this influence is mutual [1, 2]. We focus on bovine serum albumin (BSA) because the optical and biological properties of this protein are extensively studied.

Three relaxation processes named β-, γ-, and δ-relaxations are known in the absorption spectra of aqueous BSA solutions at low-frequency side (MHz–GHz frequency range) [3]. The β-relaxation, occurring in the frequency range around 10 MHz, and γ-relaxation, which is around 20 GHz, can be attributed to the rotation of the polar protein molecules in their aqueous medium and the reorientational motion of free water molecules, respectively [4]. The third δ-process, located between β- and γ-relaxations, may be attributed to bound water relaxation [3, 4]. The contribution from γ-relaxation (also responsible for hydrogen-bonded absorption) dominates in the resulting solution spectra from megahertz up to 1 THz frequency [5]. Terahertz time-domain spectroscopy has become a complementary method to study protein solutions because changes in the relative proportions of free and bound water and in relaxation properties for either of these states can all be observed in the typical 0.2–3 THz frequency range. The spectra of aqueous BSA solutions in MHz–THz frequency range do not have narrow peaks; the presence of BSA appears as a modification of broadband γ-relaxation of water. At the high-frequency side, above 10 THz, the spectroscopic response of BSA solution has narrow resonances, provided by specific molecular groups in protein molecules and their protonation state and participation in the formation of hydrogen bonds [6]. For the aqueous solution of albumin, amide III band (~ 37 THz), amide II band (~ 46 THz), amide I band (~ 50 THz), N–H, and O–H stretching bands (~ 100 THz) are observed [7].

The studies of BSA solutions in the specific terahertz range have been carried out by many scientific groups [7–12], although with different experimental techniques, solvent concentrations, and pH values. Several authors state that the absorption of BSA solutions becomes greater than that of water for concentrations lower than 17 mg/mL [9, 10], another study shows contrary results [8]. In our opinion, the use of thin (100 μm or less) solution layer in those works does not allow an accurate measurement of the complex dielectric permittivity of the sample.

To clear out this situation, we used a thicker cell and performed a thorough and detailed study of "low" BSA concentrations (1–30 mg/mL) in aqueous solutions. Our terahertz time-domain spectrometer (THz-TDS) was adapted to study low frequencies and thick water layers. To detect small-scale changes in solutions, we combined the results obtained in transmission studies in a thick cell and attenuated total internal reflection (ATR) configuration. The reliable frequency range of the obtained complex dielectric function spectrum is thus considerably broadened (0.05–3.2 THz); BSA concentrations above 10 mg/mL demonstrate reproducible and noticeable influence on the water terahertz response in the low-frequency part of the spectrum.

2 Materials and Methods

Our THz-TDS measurements, based on 100-fs, 800-nm laser pulses, were performed in two spectrometers described previously [11, 13]: a "low-frequency" spectrometer and a "high-frequency" one, see Fig. 1. Relying on our previous studies, we shifted the maximal dynamic

range of the "low-frequency" spectrometer to 0.1 THz by choosing proper emitting and detecting photoconductive antennas [14]. Special attention was paid to the lowest spectral region 0.05–0.1 THz, where the sampling range was extended to 100 ps. For the "high-frequency" spectrometer, the maximal dynamic range was shifted to 2 THz by using 0.3-mm ZnTe crystals for both emission and detection (see Fig. 1a). Two configurations were used in both spectrometers: transmission, with a cell 1000 to 100 μm thick (for low and high frequencies, respectively), and reflection configuration using a silicon prism surface (Fig. 1b). Commercially available cell holders and spacers were used; cell windows were self-made from polystyrene Petri dish base 0.7 mm thick. Polystyrene is an optimal polymer material because it is stiff enough to keep constant cell thickness, and transparent enough for the frequency range involved [15].

For the high-frequency part of spectra, the transmission configuration is not very reliable since it requires a thin cell, which means large errors, so we mainly used "low-transition," "low-reflection," and "high-reflection" configurations, Fig. 1. It is essential that the temperature and the chemical composition of albumin solutions are the same for all measurements.

The best developed method for THz-TDS solution measurements is a transmission through a thin cell [9, 10, 12]. Usually, the thickness of water layer under measurement is 50–100 μm (smaller than the wavelength!). In this case, a small variation of thickness introduces noticeable errors, especially for refraction index. Moreover, the solution properties themselves may be modified in the vicinity of the interface [16]. Hence, a thick cell is preferable. It gives considerable advantages in the low-frequency part of the terahertz spectra where water transmission is not so strongly attenuated. To avoid retro-reflections in the cell window influence, it is helpful to use the transmission of a thin solution layer ($d = 50$–100 μm) as the measurement for normalization. The only adjustable parameter for the evaluation of absorption (and refraction) spectra is layer thickness—d; in this case, it is set by a large-area teflon spacer and controlled by a micrometer. Typical uncertainty of d (after cell refilling) is 5 μm, which is critical for a 0.1-mm cell, but it is not so critical for a 0.5–1-mm cell.

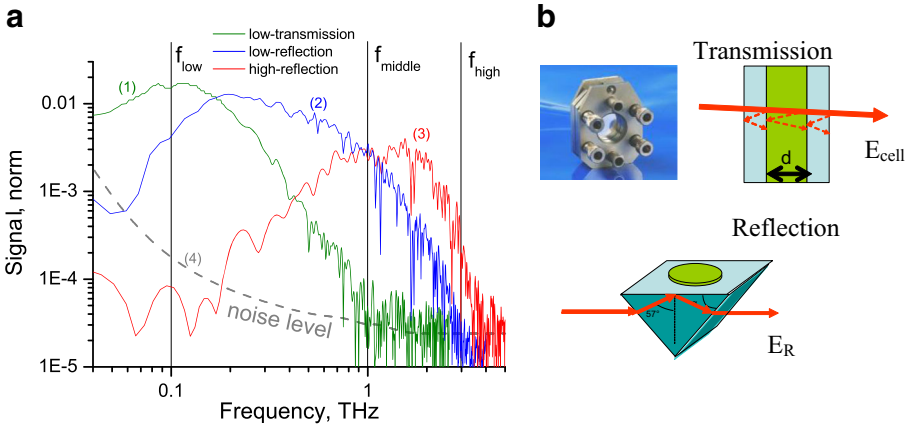

Fig. 1 (a) Experimental signal transmitted (curve 1) or reflected (curves 2, 3) for the aqueous solution of BSA, for the "low-frequency spectrometer" (curves 1, 2) and "high-frequency spectrometer" (curve 3). Vertical lines indicate particular frequencies for further analysis. Signals are normalized to the noise level (curve 4) at the high-frequency part of the spectra. (b) A sketch of the experiment: arrows indicate the path of the THz waves; d, solution layer thickness

To extract the spectra of the complex dielectric function $\varepsilon(f)$ from complex experimental transmission $T(f)$, we use the known methods [17, 18].

$$T(\omega) = E_{\text{cell\_1}}(\omega)/E_{\text{cell\_2}}(\omega) \tag{1}$$

$$\alpha(\omega) = -ln\{|T(\omega)|\}/(d_{\text{cell\_1}} - d_{\text{cell\_2}}) \tag{2}$$

where $E_{\text{cell\_}i}(\omega)$ stands for the spectra transmitted through the cell with solution layer, its thickness is $d_{\text{cell\_}i}$. $\omega = 2\pi f$ and f is the frequency in terahertz. Using normalization to $E_{\text{cell\_2}}(\omega)$, we get rid of reflection losses and retro-reflections in cell windows (see Fig. 1 b); they are identical for cell_1 and cell_2 and are canceled. Retro-reflections in a solution layer can be neglected even in the low-frequency part, since we use a thick layer in that case.

To evaluate refraction index spectra, we use:

$$n(\omega) = -arg\{T(\omega)\}\cdot c/(\omega\cdot(d_{\text{cell\_1}} - d_{\text{cell\_2}})) + 1, \tag{3}$$

And finally, we get the complex dielectric function $\varepsilon(\omega)$ as:

$$\varepsilon(\omega) = (n(\omega) - i\alpha(\omega)\cdot c/\omega)^2, \tag{4}$$

For high terahertz frequencies, ATR experiment configuration is preferable, because it does not suffer much from strong absorption by water [19–21]. Besides, the use of a prism allows us to eliminate the error associated with the thickness of water layer. Typically, ATR signal E_{R_solution} is sufficient to measure the water solution reflection spectrum in the range of 0.25–3.5 THz. The solution volume for a single measurement in the ATR configuration was 800 μL (this means a 1-mm-thick layer on the prism surface), while in the transmission configuration, it was 400 μL (for 1-mm cell thickness). For reflection normalization, we just use spectra of dry prism surface—E_{R_air}. There are two parameters to adjust for the evaluation of ATR spectra: the incidence angle θ and prism refraction n_{Si} (sensitive to ambient temperature) [17]. In addition to direct measurements, those two parameters are controlled by the best fitting to the known spectra in case of distilled water. To extract the spectra of the complex dielectric function $\varepsilon(f)$ from complex experimental reflection $R(f)$, we use the following relation [18]:

$$\varepsilon(\omega) = n_{Si}^2 \frac{(1+R(\omega)) \pm \sqrt{(1+R(\omega))^4 - \sin^2(2\theta)\left(1-R(\omega)^2\right)^2}}{2\cos(\theta)^2(1-R(\omega))^2} \tag{5}$$

where $R(\omega) = E_{R\_solution}/E_{R\_air}$, $n_{\text{Si}} = 3.41$. The reflected signal increases with frequency. Hence, reflection configuration is preferable for the high-frequency spectral region. To detect small changes in dilute solution, we normalize the solution signal to the case of distilled water—E_{R_water}.

To improve the sensitivity, we will analyze not the extracted $\varepsilon(f)$ but the most direct experimental data $T(f,C,d)$ or $R(f,C)$, normalized to the corresponding case of distilled water—$C = 0$.

$$T_{\mathrm{BSA}}/T_{\mathrm{water}}(f,C,d) = E_{\mathrm{cell}}(f,C\_\mathrm{BSA},d)/E_{\mathrm{cell}}(f,C=0,d), \tag{6}$$

$$R_{\mathrm{BSA}}/R_{\mathrm{water}}(f,C) = E_R(f,C\_\mathrm{BSA})/E_R(f,C=0), \tag{7}$$

Thus, we cancel the strong background of water absorption and dispersion, and it is easier to observe small deviations of $T_{\mathrm{BSA}}/T_{\mathrm{water}}$ or $R_{\mathrm{BSA}}/R_{\mathrm{water}}$ from 1 for low values of protein concentration C. To relate the observed changes in T or R to solution properties, we fit experimental data by the transmission or reflection, calculated from $\varepsilon(\omega,C)$ model [13]:

$$T_m(f,C,d) = T_{\mathrm{model}}(f,C,d)/T_{\mathrm{model}}(f,(C=0),d) \tag{8}$$

$$T_{model}(\omega,C,d) = \exp\left(-i\left(\left(\sqrt{\varepsilon(\omega,C)}\right)d\omega/c\right)\right) \tag{9}$$

$$R_m(f,C,d) = R_{\mathrm{model}}(f,C,d)/R_{\mathrm{model}}(f,(C=0),d) \tag{10}$$

$$R_{model}(\omega,C) = \frac{n^{*2}(\omega)\cos(\theta) - \sqrt{n^{*2}(\omega)\sin^2(\theta)}}{n^{*2}(\omega)\cos(\theta) + \sqrt{n^{*2}(\omega)\sin^2(\theta)}}, \quad n^*(\omega) = \sqrt{\varepsilon(\omega,C)}/n_{Si} \tag{11}$$

The solutions of BSA (Sigma, USA) were prepared in double-distilled water. Dry samples were weighed and dissolved in water to obtain the concentration within 1–100 mg/mL (14.5 pM–1.4 mM). To distinguish the differences at these low concentrations, the result was averaged over three independent experiments (with cell refilling and reference measurement) and for each type of measurement.

3 Results and Discussion

3.1 The Model

For the interpretation of experimental measurements, we compare them with the model. The specific feature of the terahertz spectroscopy of solutions is very strong absorption and dispersion by water itself. Actually, we do not study solute, as its contribution is negligible. We study how the solute modifies the solvent, the appearance, and the structure of hydration shell around the solute molecules. To detect small changes in the smooth spectra of the solution, we are to precisely describe solvent properties within a broad spectral range.

The most simplified but exact expression to describe the dielectric function $\varepsilon(\omega)$ of aqueous solutions within the 0.1–5-THz frequency range is a well-known two-

component relaxation (Debye) model with overdumped oscillator and conductivity additional terms [5, 11, 13, 19, 20]:

$$\varepsilon(\omega, C) = \varepsilon_\infty + \frac{\Delta\varepsilon_1(C)}{1 + (i\omega\tau_1)^\alpha} + \frac{\Delta\varepsilon_2}{1 + i\omega\tau_2} + \frac{A_1}{{\omega_{01}}^2 - \omega^2 + i\gamma_{01}\omega} + i\sigma/\omega\varepsilon_0 + \cdots \quad (12)$$

where τ_1 and τ_2 are the relaxation times for the first (main, "slow," γ-) relaxation process and the second ("fast") relaxation term, $\Delta\varepsilon_i$ are the contributions into permittivity from the first ($\Delta\varepsilon_1$) and the second ($\Delta\varepsilon_2$) terms, A_1 is the amplitude, w_{01} is the frequency, γ_{01} is the linewidth of the oscillator term, σ is the static conductivity, and ε_0 is the dielectric constant [11, 19, 20]. We suppose, that when the solute concentration C is nonzero, the only one variable parameter is $\Delta\varepsilon_1(C)$. The sum of the amplitudes of the considered terms should be equal to the precisely known static permittivity ε_s ($\varepsilon_s = 78.3$ for water at 25 °C, see Fig. 2b):

$$\varepsilon_s = \varepsilon_\infty + \Delta\varepsilon_1 + \Delta\varepsilon_2 + \frac{A_1}{{\omega_{01}}^2} + \cdots \quad (13)$$

This useful additional condition (11) fixes ε_∞ value, depending on the number of considered terms in (12).

The main term of the "slow" process is in the form of Cole–Cole model ($\alpha \leq 1$) which takes into account symmetrical broadening of the permittivity spectrum, which is observed for proteins dissolved in water [11, 24] in the gigahertz range; when $\alpha = 1$, it is simplified to Debye model [5] that is the case for distilled water, for example. In our case, $\alpha \leq 1$ improves the agreement of (12) with the experimental data for frequencies below 0.1 THz, but this improvement is not essential for our analysis, so we simplify it to $\alpha = 1$ case.

Physical processes related to the presented parameters in (12) are the following: τ_1 is assigned to the cooperative reorientation time of hydrogen-bonded (HB) bulk water molecules involving HB switching events [19, 20]. τ_2 ("fast") relaxation process can be explained by the two-fraction model of water, where a part of water is classified as non-hydrogen-bonded water isolated from the HB network, and τ_2 is assigned to the collisional relaxation of non-hydrogen-

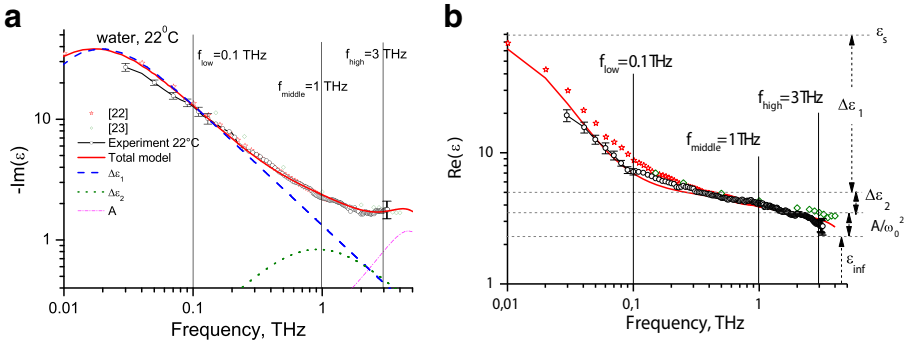

Fig. 2 **a** The imaginary part of the dielectric function of water and the contribution of each term of the model function; the selected frequencies for the concentration dependence study are 0.1, 1, and 3 THz, indicated by vertical lines. **b** The real part of the dielectric function of water. Dashed horizontal lines indicate the amplitudes of the corresponding process. The literature data from [22, 23] corresponds to 20 and 27 °C, respectively. The data are presented as the average value ± SD ($n = 3$)

bonded water [11, 25]. The noticeable sensitivity to the "fast relaxation" value is found in conductive ionic solutions [12, 26], or in water–alcohol mixtures [27]. Resonance processes correspond to several known vibrational modes in the terahertz region [28, 29]. The only significant vibrational mode for our frequency range is located at 5.3 THz.

All known processes in polar solutions below tens of terahertz are very broadband, so it is essential to combine several experimental techniques, each for its own spectral range, to obtain the spectra over many octaves. From the low-frequency side, it is well established dielectric spectroscopy [30], while from the high-frequency side, it is mostly FTIR spectroscopy [31]. When studying relaxation or overdumped oscillation processes, log–log plots of spectra are most demonstrative (Figs. 1 and 2).

To describe the dielectric function $\varepsilon(\omega)$ spectra of a protein solution, we fit the experimental complex spectra with model (12) with only the amplitude of the first relaxation term varied. We suggest that, instead of complicating the models used for the analysis of experimental data, it is necessary to improve the accuracy and repeatability of experiments and to expand the spectral range of measurements [11, 32]. We examine the three parts of the THz-TDS spectral range in detail and check the contribution from each term of model (12) into the complex dielectric function of albumin solution. We divide the available frequency range in three parts: "low" for slow relaxation dominating, "middle" for fast relaxation, and "high" for oscillator term [20, 32] (Figs. 1 and 2). From the model, we can visualize processes that dominate in each selected frequency region. At "low" frequency $f_{low} = 0.1$ THz, the contribution from the "slow" relaxation term ($\Delta\varepsilon_1$, τ_1) into total absorption ($Im(\varepsilon)$) is 98%. At the "middle" frequency $f_{middle} = 1$ THz, the contribution from the "slow" relaxation term into total absorption is 55%, the rest contribution comes from "fast" relaxation 35% and from oscillator 10%. At the "high" frequency $f_{high} = 3$ THz, the contribution from the "slow" relaxation term into total absorption is 25%; the "fast," 27%; and the oscillator, 48% (see Fig. 2a). Thus, if the changes in the terahertz response of the BSA solution are determined by the "fast" relaxation or by oscillation processes, then the best sensitivity to BSA concentration will be for "middle" or "high" frequencies. If the only change with solution properties is related to γ-relaxation, i.e., to the "slow" relaxation term, then at the frequency f_{low}, the differences of the protein solution from the solvent (water) are expected to be three to four times (98 vs 25%) stronger, as compared to the f_{high} case.

For each spectral range, a particular experimental method is the most reliable one: thick-cell transmission for "low," thin cell and ATR for "middle," and ATR for "high." Actually, all methods have considerable intersection in frequencies, so we combine the results obtained by four different methods (two spectrometers × two configurations) and thus we obtain a broader frequency range (mainly in the low-frequency side) than that typically published in THz-TDS papers on water solution spectroscopy. In all four cases, we start with the evaluation of the spectra of distilled water, until sufficient agreement with published data and with model is obtained (Fig. 2).

It follows from Fig. 2 that our data on the dielectric function of water are consistent, within the errors, with literature data [22, 23] and model (12). Previously published model [20] does not ideally describe experiments in the region below 0.1 THz; therefore, we had to modify the parameters of the slow relaxation term. We use the following parameter values [11], which do not contradict the most reliable published data: $\varepsilon_\infty = 2.3$, $\Delta\varepsilon_1 = 74.9$, $\tau_1 = 9.47$ ps, $\Delta\varepsilon_2 = 1.67$, $\tau_2 = 250$ fs, $\varepsilon_s = 78.5$; $A/\omega_0^2 = 1.14$, $\omega_0 = 5.3$ THz/2π, $\gamma_0 = 5.35$ THz/2π. Careful experimental studies of water and bio-solution dielectric function in gigahertz–terahertz range can be also found in [28, 33–35].

3.2 The Most Appropriate Fitting Parameter in the Relaxation Model

In order to investigate the dependence of the terahertz response of the solution on the concentration, a particular model parameter should be chosen, and its value should be related to the concentration value. Such model should accurately describe the change in the whole detected spectrum for this concentration. The applicability of this approach was first checked for a high (100 mg/mL) concentration of BSA. All the data on this BSA solution (from four measurement methods) were accurately combined in the form of $\varepsilon(\omega)$ and compared with water data [36]—the difference in spectra is mainly manifested in the imaginary part, at low frequencies. Such a difference is best fitted by a decrease in the amplitude of the slow relaxation amplitude $\Delta\varepsilon_1$.

An alternative approach is to use $\tau_1(C)$ as the only varied parameter instead of $\Delta\varepsilon_1$, as it was done for glucose solution [37, 38]. At frequencies above $f = 0.3$ THz, it is mathematically almost equal to vary τ_1 or $\Delta\varepsilon_1$ because $\omega\tau_1 >> 1$ and it is just a coefficient at the slow relaxation term in (12). Actually, $\Delta\varepsilon_1/\tau_1(C)$ is a more appropriate parameter to describe spectral changes at high terahertz frequencies [38], see Fig. 3a. For gigahertz frequencies for BSA solution, the changes of both $\Delta\varepsilon_1$ and τ_1 are pronounced in the experimental spectra [39, 40], but for the terahertz range we restrict only to $\Delta\varepsilon_1$ variation. In Fig. 3, we plot solution transmission normalized to the transmission of the solvent using Relations (8)–(9). In this case, the influence of cell windows and all reflections are canceled out, so it is the most stable and direct data evaluation. We demonstrate that the variation of both $\Delta\varepsilon_1$ and τ_1 can describe the presence of BSA in solution; above $f = 0.3$ THz, we cannot distinguish which parameter should be varied. But below 0.1 THz, the variation of $\Delta\varepsilon_1$ (using (1) and (8)) fits the experiment much better, which confirms the applicability of our choice. There is one more often varied parameter in dielectric function model (1)—the so-called fast relaxation term $\Delta\varepsilon_2$; its variation modifies solution spectra mostly at 0.3–2-THz frequencies. We checked whether $\Delta\varepsilon_2(C)$ can described observed experimental changes, using reflection data and Relation (10). We see in Fig. 3b that for high frequency, the variation of $\Delta\varepsilon_1$(C) fits the experiment (reflection is evaluated with (10)) quite well, while the variation of $\Delta\varepsilon_2(C)$ cannot describe the observed changes.

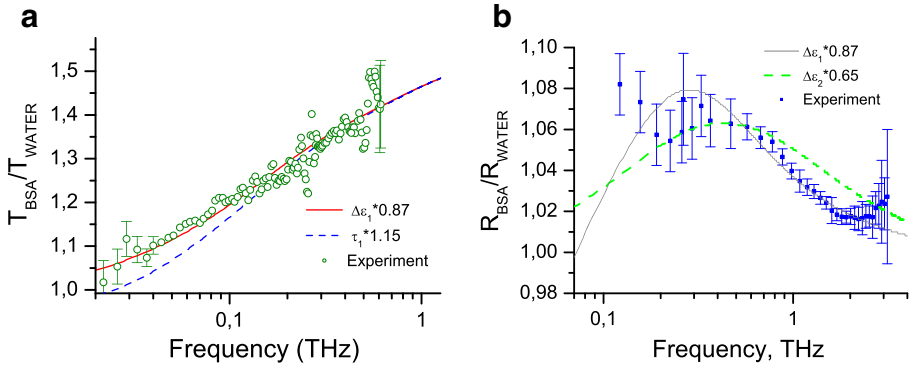

Fig. 3 **a** Transmission spectra of BSA 100 mg/mL water solution in a 500-μm cell, normalized to the case of water in the same cell; experimental data, open circles. Solid lines, model transmission (10) with the same thickness and normalization. Red line with modified $\Delta\varepsilon_1 \times 0.87$ ($\Delta\varepsilon_1/\tau_1 = 0.87$) and blue line with modified $\tau_1 \times 1.15$ ($\Delta\varepsilon_1/\tau_1 = 0.87$). **b** Reflection spectra ratio (dots) and corresponding model (12); solid line, variation of $\Delta\varepsilon_1$; dashed line, variation of $\Delta\varepsilon_2$. The data are presented as the average value ± SD ($n = 3$)

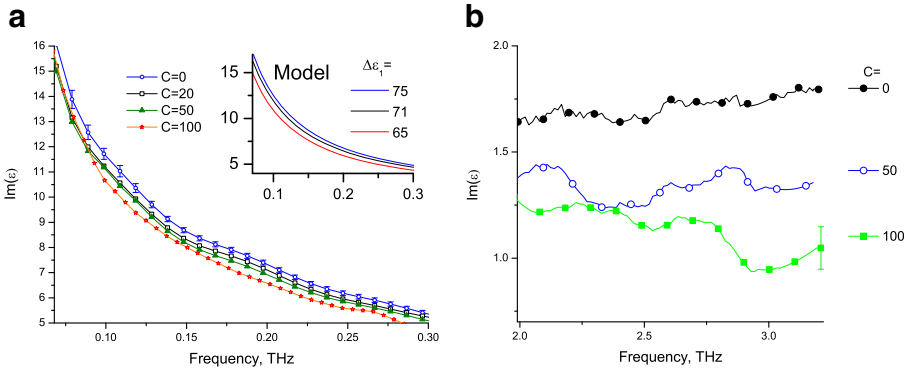

Fig. 4 **a** The low-frequency part of BSA solution $Im(\varepsilon)$ spectra for a number of concentrations (data from the transmission in 500-μm cell); on the inset, model curves of this part of the spectrum for a number of values of $\Delta\varepsilon_1$ described below. **b** The high-frequency part of the spectra of $Im(\varepsilon)$ of BSA solution from reflection data

Thus, in the whole used frequency range 0.05–3.2 THz, variation of the only one parameter $\Delta\varepsilon_1(C)$ describes solution spectra changes within our experimental error range. With this hypothesis, we will further analyze small differences in BSA solution around three selected frequencies (0.1, 1, 3 THz); the terahertz spectrum of BSA solution at concentration C will be characterized only by the value of $\Delta\varepsilon_1$ [11].

The microscopic mechanism responsible for the observed effect is the formation of bound water around solute molecules. Protein molecules themselves do not have so strong absorption and dispersion as water molecules do; we neglect the contribution from the protein itself into resulting spectra, the hydrated water shell is its contribution. It is known that the process of slow relaxation ($\Delta\varepsilon_1$) in bound water is shifted to lower frequencies ($\tau_{bounded} > \tau_1$), so that its contribution to the terahertz band becomes small [41]. The conversion of a part of the volume of water molecules from the free to the bound state is described for the terahertz range as a decrease in the amplitude of slow relaxation. Moreover, the ratio $\Delta\varepsilon_1(C)/\Delta\varepsilon_1(0)$ describes the relative volume of bound water in this simplified model.

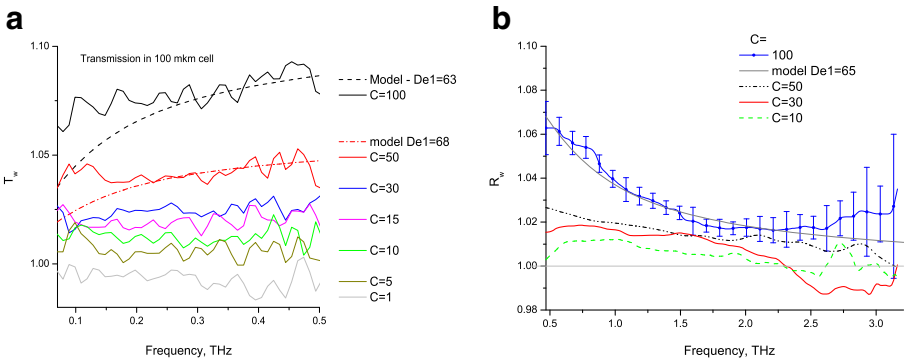

Fig. 5 **a** The ratio of the transmission amplitudes of the BSA solution to water T_w at low frequencies and a model. **b** The ratio of reflection amplitudes R_w at high frequencies

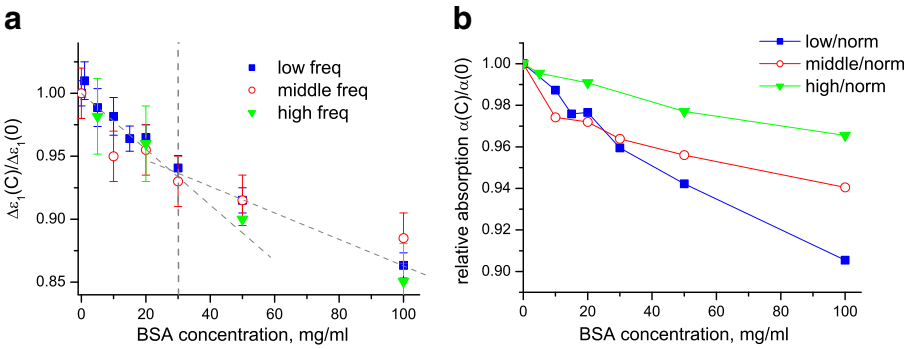

Fig. 6 **a** The dependence of slow relaxation process amplitude $\Delta\varepsilon_1$ (normalized to $\Delta\varepsilon_1$ of water) from BSA concentration in water. Data is evaluated for three frequency subregions 0.1, 1, and 3 THz. Dashed lines are to guide the eye and to mark the bend at $C = 30$ mg/mL. **b** The absorption index normalized to water absorption at corresponding frequency vs concentration

3.3 The Dielectric Function of the BSA Solution

The dielectric function, extracted from 0.5-mm cell transmission, using (1)–(4), is rather sensitive to BSA concentration only for the low-frequency part of the spectrum. Regardless of the model, we observe a decrease in $Im(\varepsilon)$ with an increase in concentration C, see Fig. 4a. We can simulate this spectral change by decreasing $\Delta\varepsilon_1$ value, see inset in Fig. 4a. This is the way in which we relate $\Delta\varepsilon_1$ to C for further analysis. We also evaluate $Re(\varepsilon)$, but it is less sensitive to BSA concentration in the terahertz range because of large constant background $\varepsilon_\infty >> Re(\Delta\varepsilon_1/(1+i\omega\tau_1))$.

For the high-frequency part of the spectrum, the extracted dielectric function (from reflection data, using(5)) is not so precise; the changes in $Im(\varepsilon)$ values are clearly distinguishable only for high BAS concentrations, starting from 50 mg/mL, see Fig. 4b.

For each concentration, we preformed three independent measurements of the sample and the reference spectra, and averaged them. The presented error is a square root of standard deviation from this mean value.

3.4 Relative Spectra Analysis

The method to relate $\Delta\varepsilon_1$ to C allows us to detect small ($C < 5$ mg/mL) BSA concentrations—see Fig. 5a. This approach describes the observed spectral changes within the whole frequency range used (0.05–3.2 THz) and for a number of concentrations from 10 mg/mL to the saturated BSA solution [11]. We perform fitting simultaneously for both parts of complex T_w or R_w, which complicates an exact agreement in a wide frequency range but increases the repeatability of the obtained $\Delta\varepsilon_1(C)$ value.

Table 1 BSA water solution properties at 22 °C

C, mg/mL	ε at 0.1 THz	ε at 1 THz	ε at 3 THz	α, cm^{-1} at 0.1 THz	α, cm^{-1} at 1 THz	α cm^{-1} at 3 THz
0	7.33-i12.5	4.151-i2.28	3.536-i1.74	79.3	227	564
30	7.21-i11.8	4.150-i2.21	3.535-i1.71	76.1	220	556
100	7.07-i10.9	4.149-i2.12	3.535-i1.68	72.3	211	547

Table 2 BSA solution published THz properties

BSA concentration (mg/mL)/in solution	Frequency, THz	The literature data	Our data (present work)	Ref
100 (1.4 mM)/10 mM NaCl, pH 7	1	$\alpha_{BSA}/\alpha_{water} = 210\ cm^{-1}/220\ cm^{-1} = 0.954$	$\alpha_{BSA}/\alpha_{water} = 211\ cm^{-1}/227\ cm^{-1} = 0.929$	9
100 (1.4 mM)/10 mM NaCl, pH 7	3	$\alpha_{BSA}/\alpha_{water} = 520\ cm^{-1}/530\ cm^{-1} = 0.98$	$\alpha_{BSA}/\alpha_{water} = 547\ cm^{-1}/564\ cm^{-1} = 0.97$	9
100/water	0.5 THz center (0.2–2)	$k/k_{water} = \alpha/\alpha_{water} = 0.93$	$\alpha/\alpha_{water} = 0.915$	37
100/water	0.5 THz center (0.2–2)	$n/n_{water} = 0.987$	$n/n_{water} = 0.990$	37
15/water	0.22–0.32	$\alpha/\alpha_{water} = 1.2$	$\alpha/\alpha_{water} = 0.90$	10
100/water	0.22–0.32	$\alpha/\alpha_{water} = 0.2$	$\alpha/\alpha_{water} = 0.97$	10
50/10 mM NaCl, pH 6	0.3–3	$\Delta\varepsilon_1/\Delta\varepsilon_{1(solvent)} = 68.2/68.73 = 0.993$	$\Delta\varepsilon_1/\Delta\varepsilon_{1(solvent)} = 69.6/74.9 = 0.93$	12

For frequencies above 2.5 THz in our setup, the signal-to-noise ratio is insufficient to determine low concentrations, but the overall trend is visible.

3.5 BSA Concentration Dependence

The idea of all our data analysis is the following: to increase the accuracy of the obtained numbers from the whole available spectrum, we need to obtain a single number that characterizes the changes in the shape and amplitude of the real and imaginary parts of the spectrum (reflection or transmission), with reasonable accuracy; for BSA solution ($C = 5$–500 mg/mL) in 0.05–3.2-THz range, the most appropriate parameter of model (12) is $\Delta\varepsilon_1$. In this way, we process the ratio of the spectra in all methods and frequencies (Fig. 5). For each concentration C (and three spectral subregions—"low," "middle," and "high"), we find one value $\Delta\varepsilon_1$ (Fig. 5). Errors of Fig. 6a are the result of averaging of three independent measurements.

Since the model is the same for the whole frequency range, the evaluated $\Delta\varepsilon_1(C)$ values for three different frequencies should coincide in Fig. 6a, although it is measured in different experiments, but the errors are less for low frequency because the sensitivity is higher there (see Fig. 3). If we present solution properties as the absorption coefficient normalized to water absorption, we see the difference in sensitivity to concentration for low and for high frequency on Fig. 6b. This confirms our suggestion that the "slow" relaxation process is the only one sensitive to BSA concentration. To simplify the comparison with other (past and future) studies, we present our data for a number of concentrations and frequencies in Table 1.

Although for increasing concentration the difference in the absolute values of absorption coefficient is maximal for the high-frequency part, the relative difference, on the contrary, is maximal for low frequency, see Fig. 6b. We also see from Table 1 that the real part of the dielectric function is much less sensitive to solute concentration than the imaginary part.

In the literature, the data on the terahertz response of BSA solution are presented in very different ways for some frequencies and for some concentrations. Since we determine $\Delta\varepsilon_1$ vs BSA concentration (see Fig. 6a) and prove the applicability of model (12) in the used parameter range, we know the BSA dielectric function for a desired frequency and concentration, so we can simulate (except pH value) relative absorption and compare it to the published experimental results, see Table 2.

Still there is a lot of contradiction in the published data, so detailed and broadband THz studies of the diluted solution of a well-known protein (BSA) should be conducted by all available methods and compared.

4 Conclusion

The dielectric properties of BSA solution were thoroughly measured within 0.05–3.2 THz using a combination of transmission and reflection methods, by optimizing the dynamic range of TDS spectrometers to low and high frequencies. We compared BSA response in three spectral subregions, around 0.1, 1, and 3 THz, and found the low-frequency part to be most sensitive to BSA concentration in water. Solution spectra were modeled by the reduction of $\Delta\varepsilon_1$, the amplitude of the "slow" or γ-relaxation process in water with increasing concentrations of the solute. This one-parameter variation describes the changes of the complex dielectric function spectra for the whole frequency range with reasonable accuracy. We have not confirmed anomalous concentration dependencies of absorption observed in other papers

[9, 10] at low BSA concentrations. The precision of our TDS method may be insufficient for the high-frequency part of THz spectra, but in no case BSA solution is more transparent than water (as it was published) for the studied frequencies and concentrations. The agreement with published data is only in following: the dependence of total absorption from the concentration of the solute is nonlinear and has a bend at the concentration about 10–60 mg/mL. We found this bend point for the case of BSA in distilled water at 22 °C to be at $C = 30 \pm 5$ mg/mL. Data in Fig. 6a for the evaluated dielectric function (at 0.05–0.3 THz) confirm this concentration bend regardless of the used models. At higher frequencies, data evaluation had to use model fitting; though our model is simplified and semi-empirical, we prove that it is valid for the broad range of frequencies and concentrations. We believe that, instead of complicating the models used for the analysis of experimental data, it is necessary to improve the accuracy and repeatability of experiments and to expand the spectral range of measurements, to increase the interaction volume and dynamic range.

Funding Information This work has been supported by the Russian Foundation for Basic Research (project no. 17-00-00275 (17-00-00270)).

Compliance with Ethical Standards

Conflict of Interest The authors declare that they have no conflict of interest.

References

1. L. Comez, M. Paolantoni, P. Sassi, S. Corezzi, A. Morresi, D. Fioretto, Soft Matter 12 (25), 5501 (2016)
2. D. Laage, T. Elsaesser, J. T. Hynes, Chem. Rev. 117, 10694 (2017)
3. N. Nandi, K. Bhattacharyya, B. Bagchi, Chem. Rev., 100 (6), 2013 (2000) DOI: https://doi.org/10.1021/cr980127v2000
4. Wolf M., Gulich R., Lunkenheimer P., Loidl A. Biochim. Biophys. Acta: Proteins Proteomics, 1824 (5), 723 (2012).
5. V. Raicu, Y. Feldman, Dielectric relaxation in biological systems: Physical principles, methods, and applications, Oxford University Press, New York, 2015.
6. A. Barth, Biochimica et Biophysica Acta 1767, 1073 (2007)
7. K. Shiraga, Y. Ogawa, N. Kondo, Biophysical Journal 111, 2629 (2016)
8. J. Xu, K. W. Plaxco, S. J. Allen, Protein Science 15 (5), 1175 (2006)
9. J.W. Bye, S. Meliga., D. Ferachou, G. Cinque, J. A. Zeitler, R. J. Falconer, J. Phys. Chem. A, 118 (1), 883 (2014)
10. O. Sushko, R. Dubrovka, R.S. Donnan, The Journal of Chemical Physics, 142, 055101–1 (2015)
11. M.M. Nazarov, O.P. Cherkasova, A.P. Shkurinov, Quantum Electronics, 46(6), 488 (2016)
12. N. Penkov, V. Yashin, E. Fesenko, A. Manokhin, E. Fesenko, Applied Spectroscopy, 72(2), 257 (2018)
13. O.P. Cherkasova, M.M. Nazarov, A.A. Angeluts, A.P. Shkurinov, Optics and Spectroscopy, 120 (1), 50 (2016)
14. M.M. Nazarov, A.P. Shkurinov, A.A. Angeluts, D.A. Sapozhnikov, Radiophysics and Quantum Electronics, 52 (18), 536 (2009)
15. E.V. Fedulova, M.M. Nazarov, A.A. Angeluts, M.S. Kitai, V.I. Sokolov, A.P. Shkurinov, Proc. SPIE 8337, Saratov Fall Meeting 2011: Optical Technologies in Biophysics and Medicine XIII, 83370I (2012)
16. N. Gorlenko, B. Laptev, G. Sidorenko, Y. Sarkisov, T. Minakova, A. Kylchenko, O. Zubkova, AIP Conference Proceedings,1698 (1), 060002 (2016)
17. M. Nazarov, A. Shkurinov, V.V. Tuchin, X.C. Zhang, Terahertz tissue spectroscopy and imaging. Handbook of photonics for biomedical science (2010).

18. A.A. Angeluts, A.V. Balakin, M.G. Evdokimov, M. N. Esaulkov, M.M. Nazarov, I.A. Ozheredov, D.A. Sapozhnikov, P.M. Solyankin, O.P.Cherkasova, A.P. Shkurinov. Quantum Electronics, 44(7), 614 (2014)
19. M. Nagai, H. Yada, T. Arikawa, K. Tanaka, International Journal of Infrared and Millimeter Waves, 27 (4), 505 (2006)
20. H. Yada, M. Nagai, and K. Tanaka, Chem. Phys. Lett 464, 166 (2008)
21. O.P. Cherkasova, M.M. Nazarov, A.P. Shkurinov, V.I. Fedorov, Radiophys. Quantum. El. 52, 518 (2009)
22. N.Q. Vinh, S.J. Allen, K.W. Plaxco, J. Am. Chem. Soc., 133 (23), 8942 (2011)
23. K. Shiraga, T. Suzuki, N. Kondo, J. De Baerdemaeker, Y. Ogawa, Carbohydr. Res., 406, 46 (2015)
24. K. Fuchs, U. Kaatze, The Journal of Physical Chemistry B, 105 (10), 2036 (2001)
25. I. Popov, P.B. Ishai, A. Khamzin, Y. Feldman, Physical Chemistry Chemical Physics, 18,13941 (2016)
26. P. U. Jepsen, H. Merbold, J Infrared Milli Terahz Waves, 31, 430 (2010)
27. S. Sarkar, D. Saha, S. Banerjee, A. Mukherjee, P. Mandal, Chemical Physics Letters, 678, 65 (2017)
28. K. Shiraga, A. Adachi, M. Nakamura, T. Tajima, K. Ajito, Y. Ogawa, The Journal of Chemical Physics, 146 (10), 105102 (2017)
29. T. Fukasawa, T. Sato, J. Watanabe, Y. Hama, W. Kunz, R. Buchner, Physical Review Letters 95 (19), 197802 (2005)
30. U. Kaatze, Journal of Chemical and Engineering Dat, 34 (4) 371 (1989)
31. M.N. Afsar, J.B. Hasted, J. Opt. Soc. Am., 67, 902 (1977)
32. O. Cherkasova, M. Nazarov, A. Shkurinov, Journal of Physics: Conference Series,793 (2017) https://doi.org/10.1088/1742-6596/793/1/012005
33. D. K. George, A. Charkhesht, N. Q. Vinh, Review of Scientific Instruments 86, 123105 (2015) https://doi.org/10.1063/1.4936986
34. U. Moller, D. G. Cooke, K. Tanaka, P. U. Jepsen, J. Opt. Soc. Am. B, 26 (9), A113(2009) doi:https://doi.org/10.1364/JOSAB.26.00A113
35. W. J. Ellison, Journal of Physical and Chemical Reference Data, 36, 1 (2007), https://doi.org/10.1063/1.2360986.
36. O.P. Cherkasova, M.M. Nazarov, A.P. Shkurinov, Proc. IEEE 41th Int. Conf. on Infrared, Millimeter, and Terahertz Waves (IRMMW-THz) (Copenhagen, Denmark, 2016). https://doi.org/10.1109/IRMMW-THz.2016.7758454
37. M. Grognot, G. Gallot, The Journal of Physical Chemistry B, 121(41), 9508 (2017)
38. K. Fuchs, U.J. Kaatze, Phys. Chem. B. 105(10), 2036–2042 (2001)
39. O. Cherkasova, M. Nazarov, A. Shkurinov, Optical and Quantum Electronics, 48(3), 217 (2016)
40. T.H. Basey-Fisher, S.M. Hanham, H. Andresen, S.A. Maier, M.M. Stevens, N.M. Alford, N. Klein, Applied Physics Letters, 99(23), 233703 (2011)
41. K. Shiraga, T. Suzuki, N. Kondo, T. Tajima, M. Nakamura, H. Togo, A. Hirata, K. Ajito, Y. Ogawa, The Journal of Chemical Physics 142 (23) 234504 (2015)